Traffic

doi:10.1111/tra.12273

A Conserved Di-Basic Motif of *Drosophila* Crumbs Contributes to Efficient ER Export

Alexandra Kumichel[1,2], Katja Kapp[1]* and Elisabeth Knust[1]*

[1]Max Planck Institute of Molecular Cell Biology and Genetics, Pfotenhauerstr.108, 01307, Dresden, Germany
[2]Present address: Membrane Traffic and Cell Division, Institut Pasteur, 28 rue du Dr Roux, 75724 Paris, France
*Corresponding authors: Elisabeth Knust, knust@mpi-cbg.de and Katja Kapp, kapp@mpi-cbg.de

Abstract

The *Drosophila* type I transmembrane protein Crumbs is an apical determinant required for the maintenance of apico-basal epithelial cell polarity. The level of Crumbs at the plasma membrane is crucial, but how it is regulated is poorly understood. In a genetic screen for regulators of Crumbs protein trafficking we identified Sar1, the core component of the coat protein complex II transport vesicles. *sar1* mutant embryos show a reduced plasma membrane localization of Crumbs, a defect similar to that observed in *haunted* and *ghost* mutant embryos, which lack Sec23 and Sec24CD, respectively. By pulse-chase assays in *Drosophila* Schneider cells and analysis of protein transport kinetics based on Endoglycosidase H resistance we identified an RNKR motif in Crumbs, which contributes to efficient ER export. The motif identified fits the highly conserved di-basic RxKR motif and mediates interaction with Sar1. The RNKR motif is also required for plasma membrane delivery of transgene-encoded Crumbs in epithelial cells of *Drosophila* embryos. Our data are the first to show that a di-basic motif acts as a signal for ER exit of a type I plasma membrane protein in a metazoan organism.

Keywords COPII, Crumbs, di-basic motif, *Drosophila*, ER export, Sar1

Received 20 December 2013, revised and accepted for publication 10 February 2015, uncorrected manuscript published online 9 March 2015, published online 14 April 2015

Crumbs (Crb) is an evolutionarily conserved type I transmembrane (TM) protein, required for apico-basal polarity, integrity of epithelial tissues, and prevention of retinal degeneration from flies to mammals (1,2). Crb proteins localize apically in epithelia and photoreceptor cells, where they organize a membrane-associated protein scaffold (1,3). The large extracellular region of most Crb proteins contains an array of epidermal growth factor (EGF)-like repeats and several laminin A G-like domains. The short, highly conserved cytoplasmic tail is characterized by a **4**.1/**E**zrin/**R**adixin/**M**oesin (FERM) domain-binding and a carboxy-terminal (C-terminal) **P**SD-95/**D**lg/**Z**O-1 (PDZ) domain-binding site (4), mediating various protein interactions. In *Drosophila*, the amount of Crb at the apical surface is crucial for cell polarity and growth regulation via the Hippo pathway. Loss of Crb can result in loss/reduction of the apical surface or enhanced tissue growth, while overexpression can lead to an increase of the apical surface (5), the induction of a second apical pole (6) or deregulated growth (7). Several mechanisms regulate Crb trafficking and stability, and thus ensure correct Crb levels at the plasma membrane. These include trafficking by exocyst (Exo84)-dependent exocytosis as well as Cdc42-, Rab11- and retromer-dependent recycling (8–13).

Trafficking of TM proteins to the surface involves the packaging into ER-derived coat protein complex II (COPII)-coated vesicles. This is mediated by specific sorting signals in the cytoplasmic regions of cargo proteins and their interaction with highly conserved COPII components (14,15). The COPII complex consists of the small GTPase secretion-associated RAS-related 1 (Sar1) as well as the heterodimeric Sec23/24 and Sec13/31 complexes. COPII coat assembly at the ER membrane and subsequent vesicle budding is initiated by the GDP/GTP exchange on Sar1 through its guanine nucleotide exchange factor Sec12. Thereby Sar1 is activated and recruits the Sec23/24 and Sec13/31 complexes, which form the inner

and outer vesicle coat, respectively (16–18). Various ER export signals in the cytoplasmic regions of cargo proteins have been identified, including di-acidic, hydrophobic and di-basic motifs (14). In most cases, cargo molecules interact with the COPII subunit Sec24 (19,20), while few cargo molecules, such as Golgi resident glycosyltransferases, directly interact with Sar1 (21).

Here, we show by *in vitro* and *in vivo* assays that *Drosophila* Crb uses a di-basic RNKR motif for efficient COPII-mediated export. This motif is sufficient to improve ER export of a reporter protein, while a di-acidic motif and the PDZ domain-binding motif are dispensable. Our results further suggest that the RNKR motif, which is highly conserved in most other Crb proteins, binds Sar1 to mediate efficient COPII-dependent ER export.

Results and Discussion

Mutations in components of the COPII complex lead to defects in Crb trafficking in embryonic epithelia

To identify regulators of Crb protein trafficking to the apical plasma membrane in *Drosophila* embryonic epithelial cells, we performed a genetic screen using a collection of deficiency lines covering the third chromosome (unpublished data). One candidate identified as a crucial component for Crb transport in many embryonic epithelial cells turned out to be the small GTPase Sar1. In wild-type epithelial cells, such as the trachea, Crb localizes to the apical plasma membrane (22) (Figure 1A-A″ arrowheads). In contrast, the majority of Crb is diffusely distributed in the cytoplasm of *sar1* mutant embryos from late stage 15 onward (Figure 1B-B″, orange arrowheads). Due to the strong maternal contribution of Sar1, zygotic *sar1* mutant embryos show a reduction, but not a complete removal of Sar1 from the trachea (23,24). This explains the residual Crb protein detected at the apical surface (Figure 1B-B″, white arrowheads) and the lack of defects in tracheal tissue morphogenesis, which is usually observed in embryos completely lacking *crb* (22). The maternal contribution of Sar1 is also sufficient for normal development of other embryonic epithelia. As a COPII component, Sar1 is involved in protein secretion and tracheal tube expansion, and its loss causes defects in cuticle formation and airway maturation as published by Tsarouhas *et al.* (23). Indeed, we also observe a reduction in tracheal tube diameter (Figure 1B). Similar but less severe defects are also seen in embryos mutant for *haunted* (*hau*) and *ghost* (*gho*) (also called *stenosis* [*sten*]), the *Drosophila* genes encoding the COPII components Sec23 and Sec24CD, respectively (25,26). As in *sar1* mutants, Crb protein accumulates in the cytoplasm of tracheal cells of stage 17 *hau* and *gho* mutant embryos (Figure 1C, C″, D and D″, orange arrowheads). The normal localization of Crb in stage 15 mutant *hau* embryos described previously (25) can be explained by the strong maternal contribution of Sec23, which allows for normal trafficking early in development, but no longer sustains Crb trafficking at later stages as shown here. For *gho* mutant embryos, our results are in agreement with published data showing a cytoplasmic accumulation of Crb in the epidermis of stage 16 *gho* mutant embryos (25). The weaker phenotype observed in *gho* mutants compared to *sar1* mutants can also be explained by the maternal contribution of Sec24CD. In addition, a second *sec24* gene, i.e. *sec24AB*, has been described in *Drosophila* (25), whose expression could also contribute to the weaker phenotype of *gho* mutants. However, to our knowledge, Sec24AB is not yet described at the protein level, especially since a well characterized mutant allele is missing. In conclusion, our results imply that Crb is trafficked from the ER in a COPII-dependent manner.

Mutation of the RNKR motif leads to trafficking defects of Crb

Classical COPII-dependent ER export motifs within the cytoplasmic tails of TM proteins include di-acidic and hydrophobic motifs as well as a di-basic motif (14,27). The inspection of the 37-amino acid long cytoplasmic tail of Crb revealed two putative classical ER export signals, a di-basic motif (RNKR) in the juxtamembrane region and di-acidic motif (EMD) located more distally. Furthermore, the short cytoplasmic tail contains a FERM domain- and a PDZ domain-binding site (Figure 2A, marked blue and orange, respectively), which have known interaction partners, e.g. Stardust for the PDZ domain-binding site. PDZ domain-containing proteins have been discussed to be involved in ER exit of their binding partners, e.g. the TM protein NR1, a subunit of the *N*-methyl-D-aspartate receptor (28), or Na^+/H^+ exchanger regulatory factor 1 and −2, which bind to the glutamate transporter GLAST at different steps during its transport to the plasma membrane (29). Thus, beside the two classical ER export motifs, the PDZ

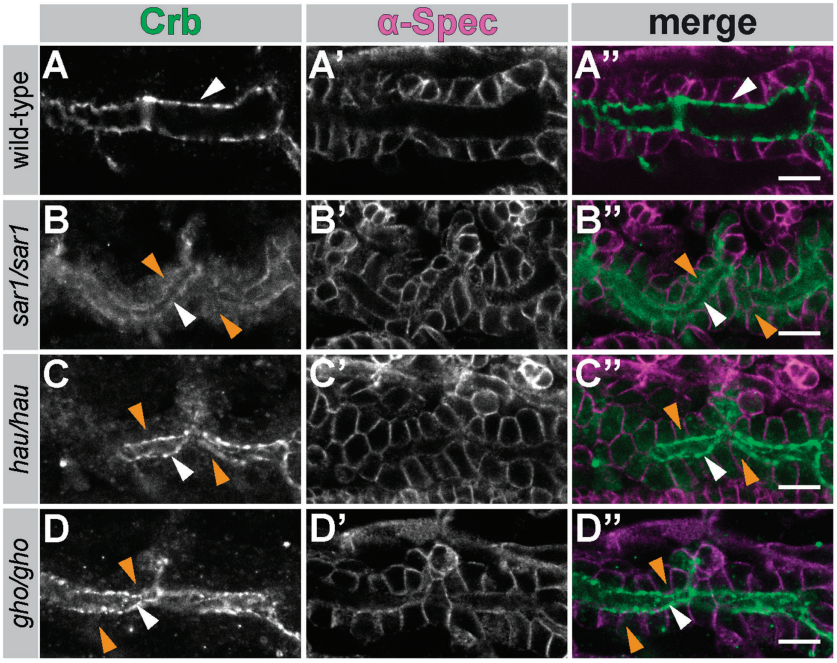

Figure 1: Mutations in *sar1*, *hau* and *gho* cause a Crb trafficking defect. (A-D″) Confocal microscopy images of stage 17 wild-type (A-A″), *sar1* mutant (B-B″), *hau* mutant (C-C″) and *gho* mutant (D-D″) embryonic trachea labeled for the polarity protein Crb (green) and the cytoskeletal component α-Spectrin, marking the cell outlines (magenta). Scale bars: 10 μm. White arrowheads mark the apical surface, orange arrowheads the cytoplasm.

domain-binding site might also be involved in ER export. Interestingly, all three motifs are highly conserved in most Crb proteins from *Drosophila* to vertebrates (Figure 2B).

To determine which of the motifs is required for ER export of Crb, we analyzed protein transport kinetics. In mammalian cell culture systems this approach is often based on the Endoglycosidase H (Endo H) resistance of overexpressed wild-type and mutant variants. Endo H cleaves high mannose *N*-glycans (containing at least three mannose moieties) and some hybrid type but not complex *N*-glycans as found in the late Golgi. Thus, Endo H resistance is characteristic for proteins that have already passed the early Golgi (30,31). *Drosophila* is known to form predominantly high mannose and paucimannose glycans, which might be core-fucosylated (32). Endo H resistance of fly proteins has been shown to occur, e.g. for VIP36 expressed in *Drosophila*-derived SL-3 cells (33). Here, we adopted a pulse-chase experiment using *Drosophila* Schneider ($S2R^+$) cells overexpressing wild-type Crb as well as variants carrying mutations in the putative ER exit motifs, and analyzed Endo H resistance.

The constructs used encode a minimized version of Crb, named Crb-short, in which the extracellular region is reduced to the signal sequence and the two C-terminal EGF-like repeats, which carry four potential *N*-glycosylation sites, followed by the TM region and the cytoplasmic tail. To detect these proteins, an HA-tag was introduced N-terminal to the EGF-like repeats. Based on a wild-type version, called HA-Crb-short^{RNKR}, single and double mutants in the putative export motifs were generated, called HA-Crb-short$^{RNKR>MNEP}$, HA-Crb-short$^{EMD>AMA}$, HA-Crb-short^{double} and HA-Crb-short$^{\Delta ERLI}$ (Figure 2C). To assess transport kinetics in the early secretory pathway of wild-type and mutant HA-Crb-short proteins, $S2R^+$ cells expressing the respective proteins were metabolically labeled, chased for different time intervals and lysed. Proteins were treated with Endo H and analyzed by gel electrophoresis and autoradiography. At time point 0, a portion of pulse labeled HA-Crb-short^{RNKR} (wild-type) exhibits Endo H resistance (Figure 2D, the two protein fractions are termed resistant [r] and sensitive [s], respectively). After 90 and 180 min chase intervals, metabolically labeled HA-Crb-short^{RNKR} achieves almost full Endo H resistance, demonstrating that most of the labeled protein has left the ER and reached the Golgi. In contrast, mutant HA-Crb-short$^{RNKR>MNEP}$ shows reduced Endo H resistance after 90 or 180 min chase intervals (Figure 2D). Quantification of Endo H resistance in six independent experiments revealed that only about 67% of mutant HA-Crb-short$^{RNKR>MNEP}$ protein is Endo H resistant after 180 min chase, in comparison to about

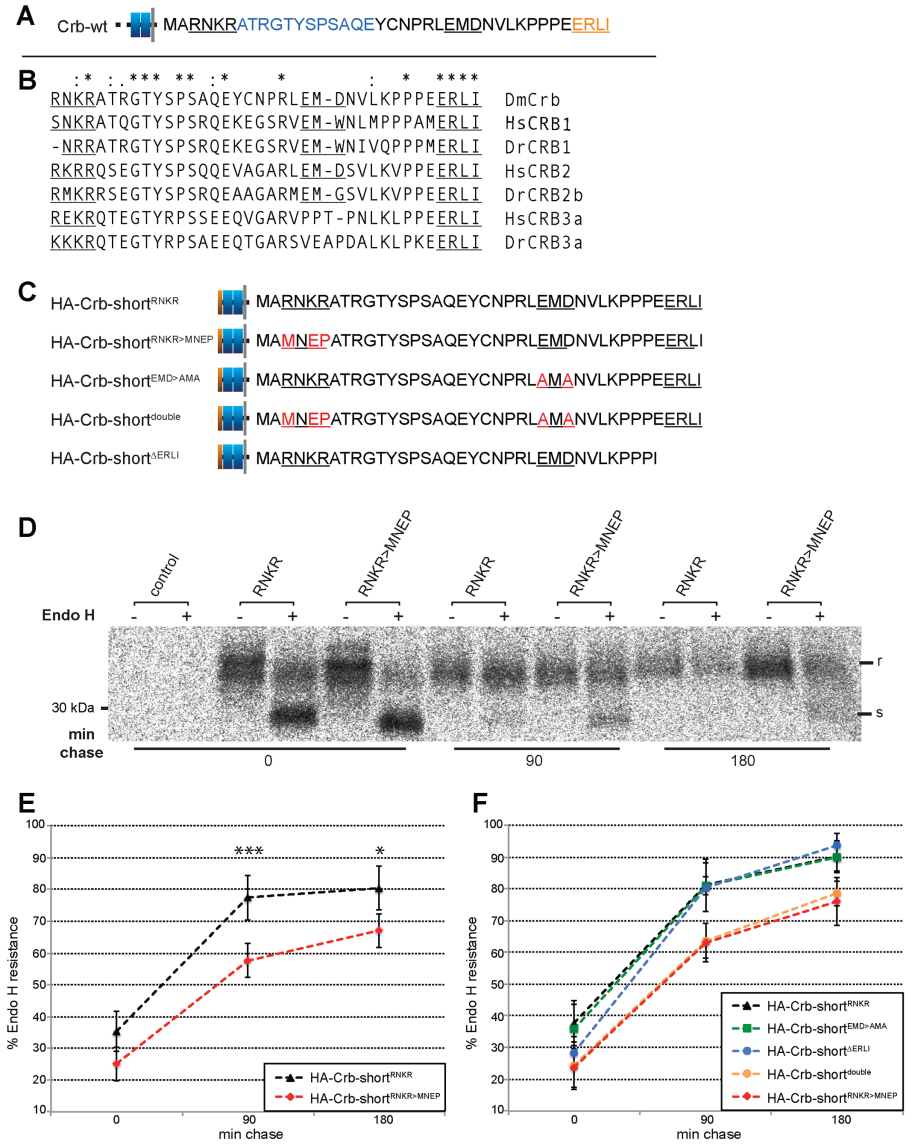

Figure 2: The RNKR motif is necessary for efficient ER export of HA-Crb-short^{RNKR}. (A) Schematic representation of the Crb cytoplasmic tail with the FERM domain-binding motif in blue and the PDZ domain-binding motif in orange. (A–C) The underlined letters correspond to the RNKR, the EMD and the ERLI motif. (B) A ClustalW multiple sequence alignment of Crb cytoplasmic tails of *Drosophila melanogaster* (*Dm*Crb, P10040) together with different Crb proteins from *Homo sapiens* (*Hs*CRB1, P82279; *Hs*CRB2, Q5IJ48; *Hs*CRB3, Q9BUF7) and *Danio rerio* (*Dr*CRB1, Q1A5L3; *Dr*CRB2b, Q1A5L1; *Dr*CRB3a, Q1A5L0). (C) The Crb variants used in this study. Brown rectangle: HA-tag, blue rectangles: EGF-like repeats, gray bar: TM region. Red letters in the amino acid sequences indicate exchanges. (D) S2R$^+$ cells expressing HA-Crb-short^{RNKR} or HA-Crb-short$^{RNKR>MNEP}$ were pulse labeled for 60 min and chased for the times indicated. Transport to the Golgi was measured by appearance of Endo H resistant protein (r) in relation to Endo H sensitive protein (s). (E) Quantification of Endo H resistance of HA-Crb-short^{RNKR} and HA-Crb-short$^{RNKR>MNEP}$. The values are means ± standard deviation of six independent experiments. $^{*}p \leq 0.01$ versus wild-type *t*-test; $^{***}p \leq 0.001$ versus wild-type *t*-test. (F) Quantification of Endo H resistance of HA-Crb-short^{RNKR}, HA-Crb-short$^{EMD>AMA}$ and HA-Crb-short$^{\Delta ERLI}$ as well as HA-Crb-short^{double} and HA-Crb-short$^{RNKR>MNEP}$. The values are means ± standard deviation of three independent experiments. The *t*-test comparing wild-type versus HA-Crb-short$^{RNKR>MNEP}$ revealed $p \leq 0.01$ at each time point. The *t*-test comparing wild-type versus HA-Crb-short^{double} revealed $p \leq 0.05$ at 0 and 90 min and $p \leq 0.01$ at 180 min.

80% of wild-type HA-Crb-short^{RNKR} protein (Figure 2E). To analyze the role of the di-acidic motif (EMD), the di-acidic motif in combination with the di-basic motif (double mutant), and the PDZ domain-binding site ERLI, we expressed HA-Crb-short$^{EMD>AMA}$, HA-Crb-short^{double} and HA-Crb-short$^{\Delta ERLI}$ (Figure 2C) and measured their Endo H resistance in pulse-chase experiments. Strikingly, no decreased Endo H resistance is observed for HA-Crb-short$^{EMD>AMA}$ or HA-Crb-short$^{\Delta ERLI}$ compared to wild-type HA-Crb-short^{RNKR}. At 180 min chase, only the mature, Endo H-resistant proteins are detected after Endo H treatment, similar as described for the wild-type protein (Figure 2F). In contrast, HA-Crb-short^{double} shows the same reduced Endo H resistance as the singly mutated protein HA-Crb-short$^{RNKR>MNEP}$ (Figure 2F).

To our knowledge, these results are the first obtained using Endo H resistance of a *Drosophila* protein as a tool to measure transport kinetics. By this, we could demonstrate that the conserved di-basic RNRK motif plays a vital role for the efficient exit of the type I plasma membrane protein Crb from the ER, while the di-acidic motif and the PDZ domain-binding site are not required under these experimental conditions. The high conservation of this di-basic RxKR motif in most vertebrate Crb proteins (Figure 2B) suggests an evolutionary conserved function. So far, a di-basic motif was shown to act as an ER export signal for Golgi-resident glycosyltransferases, which are type II membrane proteins (21). A di-basic sorting motif together with a di-leucine motif is required for the COPII-dependent ER export of a phosphotransferase subunit, which is a type III membrane protein (34). Finally, an RRR motif is required for the ER exit of the α_{2B}-adrenergic receptor, a seven TM protein (35). Thus, our finding of the influence of a di-basic motif for the exit of a type I plasma membrane protein is a further example for a more general role of this motif in ER export.

The observation that a large fraction of the mutant HA-Crb-short$^{RNKR>MNEP}$ protein was still transported out of the ER suggests that the RNKR motif is not the only export signal required under these experimental conditions. However, our results excluded the di-acidic motif and the PDZ-domain binding region. Additional, conserved or novel, motifs in the TM region or the cytoplasmic tail may be required for efficient Crb export. A possible motif is an RL-dipeptide, a sequence, which was recently identified as an ER export signal in the rat γ-aminobutyricacid transporter-1 (36). Two RL-dipeptides are also present in the Crb cytoplasmic tail. Other proteins use unique signals, such as the Kit ligand, whose efficient ER export relies on a valine residue in the C-terminus of its cytoplasmic domain (37). Therefore, it is not unlikely that more than one ER exit signal is involved in the efficient ER export of Crb.

A mutated RNKR motif affects efficient Crb trafficking in embryonic epithelial cells

In order to test whether the RNKR motif in the HA-Crb-short cytoplasmic tail is also essential for ER export in *Drosophila*, we generated transgenic flies carrying UAS-constructs encoding HA-Crb-short^{RNKR} or HA-Crb-short$^{RNKR>MNEP}$. First, we expressed both proteins in embryonic tracheal cells using the *btl*-GAL4 driver line in otherwise wild-type embryos. Immunohistochemistry of stage 16 embryos revealed that the majority of HA-Crb-short^{RNKR} localizes at the plasma membrane together with the membrane marker α-Spectrin (Figure 3A-A″ white arrowheads). In contrast, HA-Crb-short$^{RNKR>MNEP}$ is predominantly visible in the cytoplasm of the tracheal cells (Figure 3B-B″ orange arrowheads), but hardly detectable at the plasma membrane (Figure 3B and B″ white arrowheads). To confirm our data in a different cell type, we also analyzed both transgene-encoded proteins in the amnioserosa cells of stage 13–14 embryos, using the ubiquitously expressing *da*G32-GAL4 line (Figure 3C-F). In these relatively big cells, the majority of HA-Crb-short^{RNKR} localizes to the plasma membrane, where it colocalizes with the membrane marker α-Spectrin (Figure 3C-C″ white arrowheads). Only some protein is detected intracellularly (Figure 3C and C″ orange arrowheads). In contrast, HA-Crb-short$^{RNKR>MNEP}$ is predominantly visible in the cytoplasm of the amnioserosa cells (Figure 3D-D″ orange arrowheads), but hardly visible at the plasma membrane (Figure 3D and D″ white arrowheads). To identify the intracellular compartment, to which both proteins localize, we used an antibody that recognizes the KDEL signal, necessary for retrograde protein transport from the Golgi and therefore considered as an ER marker. Most of the intracellular pool of both HA-Crb-short^{RNKR} and HA-Crb-short$^{RNKR>MNEP}$ colocalize with the KDEL signal

(Figure 3E-F″ orange arrowheads), confirming their localization in the ER. The presence of some HA-Crb-short^{RNKR} protein in the ER could be explained by GAL4-mediated overexpression of the protein.

To summarize, the RNKR motif of the Crb cytoplasmic tail is necessary for efficient ER export not only in S2R$^+$ cells, but also in embryonic epithelia, such as tracheal and amnioserosa cells. Thus, the function of a di-basic ER export motif in a *Drosophila* type I TM protein can be shown in the physiological context of the organism. The results are supported by the observation that the truncated Crb protein encoded by the allele *crb^{8F105}* localizes at the apical plasma membrane in some epithelial cells that maintain their polarity, e. g. the boundary cells in the embryonic hindgut (38). The protein encoded by this allele retains the N-terminal 14 amino acids of the cytoplasmic domain, including the RNKR motif, but lacks the EMD and the ERLI motif (including one RL di-peptide) as well as an additional RL-dipeptide harbored between the FERM- and PDZ-domain-binding sites (4). Therefore, the di-acidic EMD-, the RL- and the ERLI motif can be excluded as crucial ER export signals, not only in S2R$^+$ cells but also in embryonic epithelial cells. Furthermore, a Crb-short version with the entire cytoplasmic region replaced by GFP, thus missing the RNKR motif, predominantly localizes to the ER upon overexpression in S2R$^+$ cells and amnioserosa cells (data not shown), which strengthens the role of the RNKR motif for efficient ER export.

The RNKR motif is also functional in a reporter protein context

In order to test whether the identified ER export motif is also functional in a different protein context, we designed two reporter constructs. They encode the extracellular and TM-region of CD2, followed by the wild-type or the mutated RNKR motif fused to GFP, and are named CD2$^{RNKR\text{-}GFP}$ and CD2$^{MNEP\text{-}GFP}$, respectively (Figure 4A). CD2, as a heterologous membrane marker (39), contains three potential *N*-glycosylation sites. The proteins were expressed in S2R$^+$ cells, and Endo H resistance of metabolically labeled CD2 proteins was monitored at two different chase time points (30 and 180 min; Figure 4B and C). Without Endo H treatment, four bands are detected in cells expressing CD2$^{RNKR\text{-}GFP}$ and CD2$^{MNEP\text{-}GFP}$ after 0, 30 and 180 min chase. The fastest migrating band probably corresponds to the non-glycosylated protein, as it co-migrates with fully deglycosylated protein after Endo H treatment (Figure 4B; [s]). The slower migrating bands (Figure 4B; 1 – 3) probably correspond to mono-, di- and tri-glycosylated proteins, respectively. Upon Endo H treatment of either protein, predominantly fully deglycosylated proteins were detected, indicating that the majority of CD2$^{RNKR\text{-}GFP}$ and CD2$^{MNEP\text{-}GFP}$ has not yet obtained a Golgi-dependent modification of their glycans (Figure 4B, time point 0 and 30 min). After 180 min chase less CD2$^{MNEP\text{-}GFP}$ is Endo H resistant compared to CD2$^{RNKR\text{-}GFP}$ (Figure 4B). The difference observed between the Endo H resistance of CD2$^{RNKR\text{-}GFP}$ and CD2$^{MNEP\text{-}GFP}$ after a 180-min chase is very small, but significant (Figure 4C). A similar difference in Endo H resistance was observed after a 90- and 360-min chase period (data not shown). Interestingly, the Endo H-resistant protein (r) migrates faster than the tri-glycosylated one (Figure 4B, 180 min chase, band 3). This may be due to strong trimming of the *N*-glycans in the Golgi. This is supported by the observation that after 360 min chase, the majority of non-treated proteins co-migrate with Endo H resistant proteins (data not shown). The results obtained suggest that the RNKR motif introduced into a reporter protein also improves ER exit. The rather small effect of the RNKR motif on the transport of the reporter is either due to the fact that this motif is not fully recognized in this particular context, or suggests that the RNKR motif alone is not a very strong signal, or a combination of both.

The cytoplasmic tail of Crb interacts with Sec24CD

In most cases studied, cargo selection by the COPII machinery is mediated by the Sec24 subunit (19,20). In order to find out whether the RNKR motif of Crb is required for the interaction with the COPII complex, we co-expressed an EGFP-tagged version of Sec24CD together with either HA-Crb-short^{RNKR} or any of the HA-Crb-short mutant proteins described above (Figure 2C). Following a successful co-overexpression in S2R$^+$ cells, complexes were immunoprecipitated from cell lysates with an anti-HA antibody and analyzed by Western Blot using an anti GFP-antibody (Figure 5A, top panel). The wild-type HA-Crb-short^{RNKR} as well as all mutant versions of the protein could precipitate EGFP-Sec24CD, showing that Sec24CD can interact with

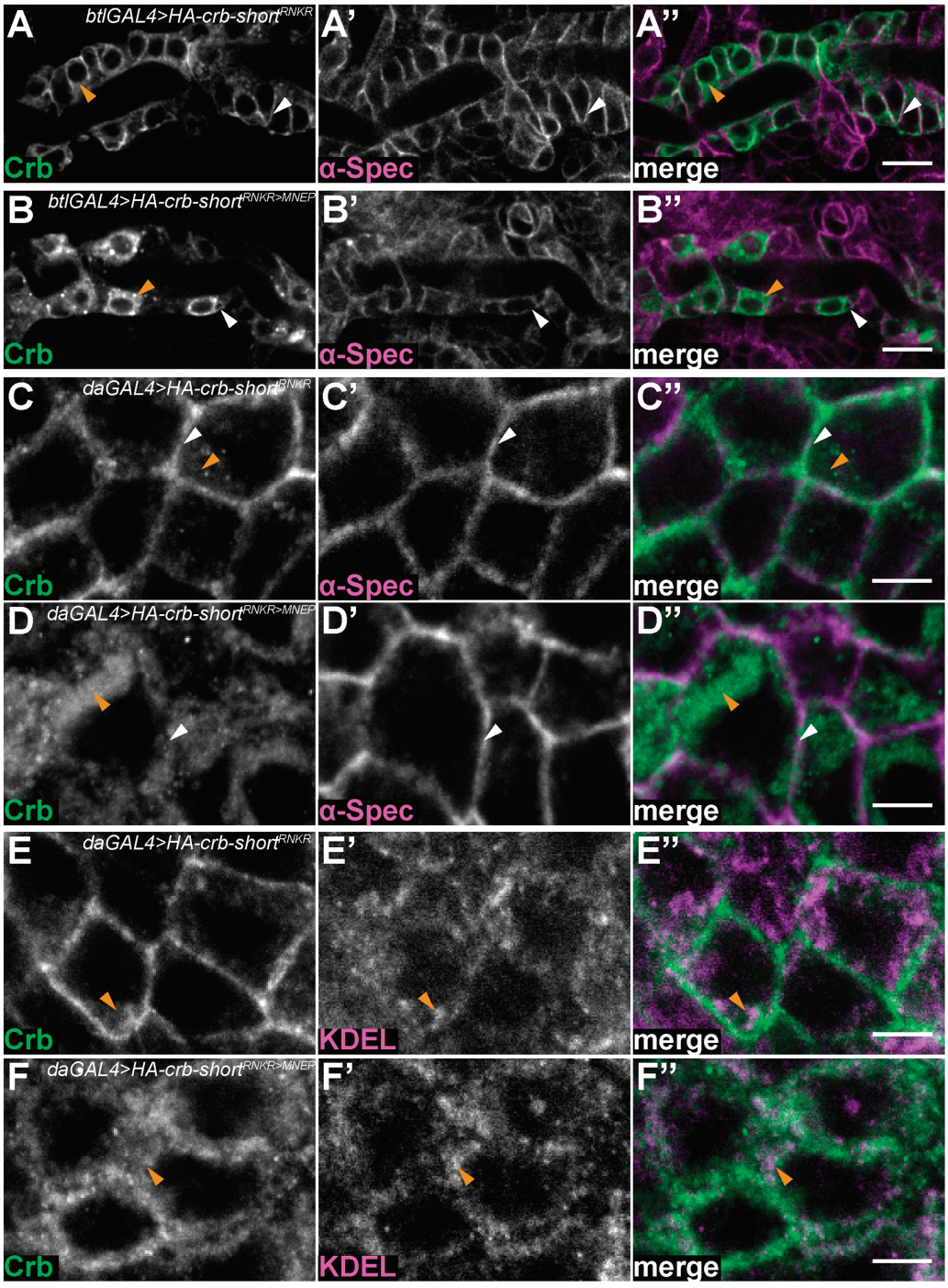

Figure 3: HA-Crb-short$^{RNKR>MNEP}$ shows impaired traffic to the plasma membrane in embryonic epithelial tissues. (A-B″) Confocal microscopy images of tracheal epithelial cells of stage 16 embryos expressing *HA-crb-short*^{RNKR} (A-A″) or *HA-crb-short*$^{RNKR>MNEP}$ (B-B″) under the control of *btl*-GAL4. Embryos were stained with anti Crb-intra (green) and anti α-Spectrin (magenta), marking the cell outlines. (C-F″) Confocal microscopy images of amnioserosa epithelial cells of stage 13–14 embryos expressing *HA-crb-short*^{RNKR} (C-C″ and E-E″) or *HA-crb-short*$^{RNKR>MNEP}$ (D-D″ and F-F″) under the control of *daG32*-GAL4. (C-D″) Embryos were stained with anti Crb-intra (green) and anti α-Spectrin (magenta) (C′, C″, D′, D″) and the ER marker KDEL (magenta) (E′, E″, F′, F″). Scale: 10 μm (A-B″); 5 μm (C-F″). White arrowheads mark the cell outlines, orange arrowheads the cytoplasm.

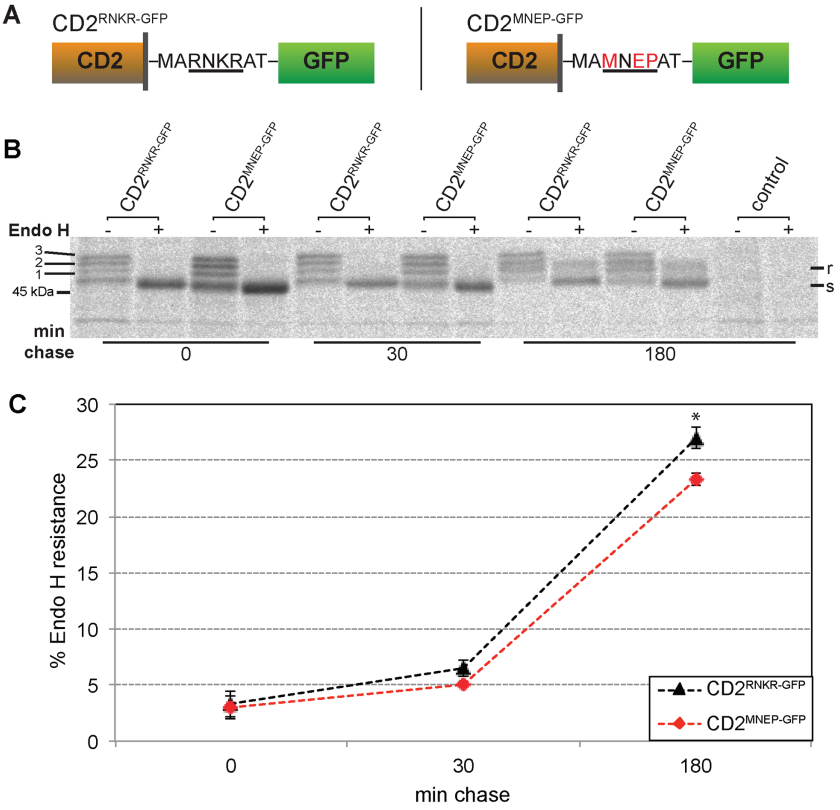

Figure 4: The RNKR motif is functional in the CD2-reporter construct. (A) Schematic representation of the reporter constructs consisting of the extracellular (brown rectangle) and TM (gray bar) region of CD2, followed by the wild-type or mutated motif and GFP (green rectangle). (B) S2R$^+$ cells expressing CD2$^{RNKR-GFP}$ and CD2$^{MNEP-GFP}$ were pulse labeled for 30 min and chased for the times indicated. Transport to the Golgi was measured by the presence of Endo H resistant protein (r) in relation to Endo H sensitive protein (s). (D) Quantification of Endo H resistance of CD2$^{RNKR-GFP}$ and CD2$^{MNEP-GFP}$ in three independent experiments. *$p \leq 0.01$ versus wild-type *t*-test.

the cytoplasmic tail of Crb regardless of the mutations in the putative ER export motifs. Interestingly and comparable to our results, the above mentioned RRR motif of the mammalian α_{2B}-adrenergic receptor was shown to preferentially interact with Sec24C and Sec24D rather than Sec24A or Sec24B (35).

The RNKR motif mediates the interaction with GST-Sar1

As binding of Sec24CD was not largely affected by mutations in the RNKR motif, we further analyzed the role of the di-basic motif for a possible COPII interaction. In vertebrate glycosyltransferases a di-basic ER export motif has been reported to directly bind to the small GTPase Sar1 (21). To test whether the di-basic ER export motif of Crb interacts with *Drosophila* Sar1, S2R$^+$ cell lysates containing either HA-Crb-short^{RNKR} or HA-Crb-short$^{RNKR>MNEP}$ were incubated with recombinant GST-tagged Sar1^{H74G}, which is the active GTP-locked mutant (40). Protein complexes were analyzed by glutathione-sepharose pull-down and Western blotting. GST-Sar1^{H74G} pulled down some HA-Crb-short^{RNKR} (Figure 5B, lane 5), but not HA-Crb-short$^{RNKR>MNEP}$ (Figure 5B, lane 6). Thus, the RNKR motif in the cytoplasmic tail of Crb could potentially mediate the interaction between Crb and the COPII complex via Sar1 in order to increase transport efficiency.

Beside the vertebrate glycosyltransferases mentioned above, Sar1 is known to directly interact with cargo proteins such as yeast Bet1 (21,41), suggesting that direct binding is a more common phenomenon. The rather weak interaction between GST-Sar1^{H74G} and HA-Crb-short^{RNKR} could be due to the fact that the interaction requires co-factors whose amounts and/or activity are limited in this experimental system. Alternatively, GST-Sar1^{H74G} or HA-Crb-short^{RNKR} may bind strongly to other proteins present in the lysate. Beyond that, the weak interaction might result from the lack of membranes, which usually provide the physiological environment and promote interactions.

In summary, we have shown that the RNKR motif in Crb contributes to the ER export by interactions with Sar1. This is the first example of the role of a di-basic motif as ER export signal in a *Drosophila* type I membrane protein. We further show that this sequence is functional in a

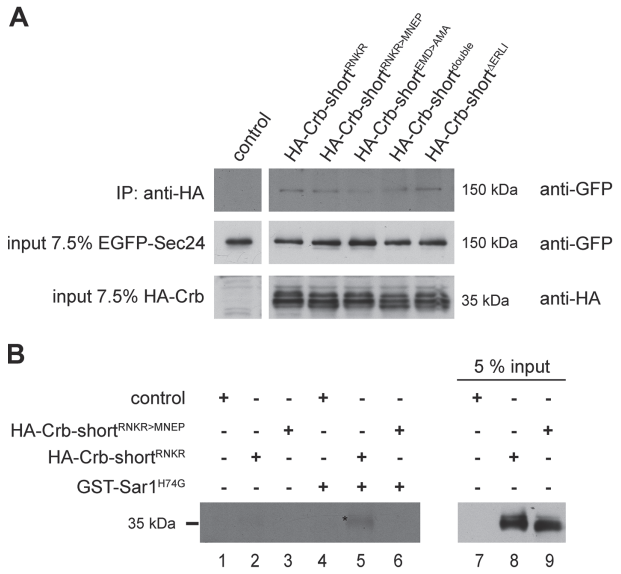

Figure 5: The cytoplasmic tail of Crb interacts with the COPII machinery. (A) EGFP-Sec24CD interacts with HA-Crb-short^{RNKR}, HA-Crb-short$^{RNKR>MNEP}$, HA-Crb-short$^{EMD>AMA}$, HA-Crb-short^{double} and HA-Crb-short$^{\Delta ERLI}$, shown by co-immunoprecipitation and Western Blot analyses. S2R^{+} cells expressing EGFP-Sec24CD together with GFP (control), HA-tagged Crb-short^{RNKR}, Crb-short$^{RNKR>MNEP}$, Crb-short$^{EMD>AMA}$, HA-Crb-short^{double} or Crb-short$^{\Delta ERLI}$ were lysed and the Crb variants were immunoprecipitated with anti HA-antibody. Immunoprecipitates were separated by SDS-PAGE and Sec24CD was determined by immunoblotting using anti GFP-antibody (upper panel). Lower panels show the input controls of EGFP-Sec24CD and the HA-tagged Crb variants, probed with anti-EGFP and anti-HA antibody, respectively. (B) Lysates from S2R^{+} cells expressing HA-Crb-short^{RNKR}, HA-Crb-short$^{RNKR>MNEP}$ or mock-transfected (control) were incubated with glutathione-sepharose beads with GST (lane 1–3) or in the presence of recombinant GST-Sar1^{H74G} (lane 4–6). After incubation, beads were washed and bound complexes analyzed by SDS-PAGE and Western blotting with anti-HA antibody. Lanes 7–9 serve as input control. The asterisk in lane 5 marks the band.

physiological context of the organism. Recently, *Drosophila* has become more important for the analyses of the early secretory or endocytic pathway in the context of cell polarity and development (reviewed in 42, 43). In comparison to vertebrates, which often have multiple copies of protein transport components, the fly typically has less or just a single copy of each. This makes *Drosophila* an ideal model to study the regulation of the early steps of the secretory pathway under physiological conditions (42,43). These studies will contribute not only to our understanding of cell polarity and development (43), but may also help to unravel the origin of diseases associated with defects in the early secretory pathway such as chylomicron retention disease or Anderson's disease caused by mutations in human Sar1B (44). In the future, it will be interesting to investigate, how Crb travels from the ER to the apical plasma membrane, which includes to understand which additional motif(s) and/or features may be required for ER exit and apical membrane targeting.

Materials and Methods

Fly stocks

Flies were kept at 18 or 25°C and staged according to the time of development described in Campos-Ortega and Hartenstein (45). The following stocks were obtained from the Bloomington stock center: OregonR as wild type control, *sar1^{05712}*, *sec23^{9G}*, *gho^{1}*, *daG32-GAL4*, *and btlGAL4*. The mutant stocks were balanced over *TM3*, *twist-GAL4*, *UAS-EGFP* or *Cyo*, *twist-GAL4*, *UAS-EGFP*. The following stocks were generated in this study: *UAS-HA-crb-short^{RNKR}*, *UAS-HA-crb-short$^{RNKR>MNEP}$*. Transgenic flies were generated using the phiC31 integrase mediated site-specific integration into attP landing-sites (46). For the injection and establishment of transgenic lines, standard protocols were followed (47). *UAS-HA-crb-short^{RNKR}* and *UAS-HA-crb-short$^{RNKR>MNEP}$* were integrated into the landing site *attP3A* of the stock *y M(vas-int.DM) ZH-2A w; PBac (y^{+} attP-3B) VK00001* (Bloomington No. 24861).

Antibodies

Primary antibodies used: rabbit anti-Crb-intra 2662, (1:400, raised against the peptide NKRATRGTYSPSAQE), rat anti-Crb 2.8 (1:1000) (48), rabbit anti-GFP (Life Technologies), mouse anti-HA antibodies (HA.11 Clone 16B12, Covance), mouse anti-KDEL (1:300) (Stressgen), mouse anti-α Spectrin 3A9 (1:400) (DSHB).

Plasmids

To clone the Crb-short construct, the cDNA sequence representing the 28th and 29th EGF-like repeat, the TM region, the cytoplasmic tail and the 3′UTR of Crb^{wt} (5) was amplified by PCR using the primers (5′-ATAGATCTGACATCGACGAGTGCAAC-3′ and 5′-CGGTCTAGA GCAAAATATGTTTTTTATTTG-3′) including the restriction sites BglII and XbaI. The PCR product was cloned into the Crb^{intra} construct (5), replacing the TM region, cytoplasmic tail and 3′UTR of this construct. The HA-tag was inserted by overlap-extension PCR using the primers (5′-TACTGAAATCTGCCAAGA-3′; 5′-AGCGTA ATCTGGAACATCGTATGGGTACGTCGGCACCGCCACTGAGG-3′;

5′-TACCCATACGATGTTCCAGATTACGCTGAGGAGGCGTACTTT AATGGCT-3′ and 5′-GTTTGTCCAATTATGTCA-3′). Thus, the construct includes the Crb 5′ and 3′UTR, and encodes the signal sequence, the HA-tag, the 28th and 29th EGF repeat, the TM, and the cytoplasmic region. The constructs with the mutations were also cloned by overlap-extension PCR using the primers (5′-TACTGAAATCTGC CAAGA-3′; 5′-TGGGCACCTTCCTGGTGATGGCCATGAACGAGCC AGCAACCAGGGGCACCTATAGCC-3′; 5′-GGCTATAGGTGCCCCT GGTTGCTGGCTCGTTCATGGCCATCACCAGGAAGGTGCCCA-3′ and 5′-GTTTGTCCAATTATGTCA-3′) for HA-Crb-short$^{RNKR>MNEP}$ and (5′-TACTGAAATCTGCCAAGA-3′; 5′-GCTTCAGTACGTTGGCC ATTGCCAGCCGTGGG-3′; 5′-GCTTCAGTACGTTGGCCATTGCC AGCCGTGGG-3′ and 5′-GTTTGTCCAATTATGTCA-3′) for HA-Crb-short$^{EMD-AMA}$, respectively. The overlap-extension product was amplified with the primers (5′-TACTGAAATCTGCCAAGA-3′ and 5′-GTTTGTCCAATTATGTCA-3′) and cloned into the pUASTattB vector (49). For the double mutant, the single mutant was used to insert the second mutation by a second round of overlap-extension PCR. The construct Crb-short$^{\Delta ERLI}$ was generated by site-directed mutagenesis of the wild-type version using the primers 5′-CCACCGCCGATATAGCGACT AATTTAGTTTTG-3′ and 5′-CAAAACTAAATTAGTCGCTATATCGG CGGTGG-3′, to insert an isoleucine residue followed by a premature stopcodon. Thus, the construct resembles the construct Myc-Intra$^{\Delta ERLI}$ used in Klebes & Knust (4).

For the CD2$^{RNKR-GFP}$ and CD2$^{MNEP-GFP}$ fusion constructs, the CD2-Crbintra (4) construct was used as matrix and was amplified with the primers (5′-GTTTGTCCAATTATGTCA-3′ and either 5′-CTCA CCATGGTGGCGCTAGCGCCCCCAACGGTTGCTCGCTTGTTCCT GGCCATGCAGATACAGAAAATAAACAGCGCCCC-3′ for CD 2$^{RNKR-GFP}$ or 5′-CTCACCATGGTGGCGCTAGCGCCCCCAACGGTT GCTGGCTCGTTCATGGCCATGCAGATACAGAAAATAAACAGCG CCCC-3′ for CD2$^{MNEP-GFP}$) thereby adding the DNA sequence encoding 'MARNKRAT' or 'MAMNEPAT' to the CD2 extracellular and TM region. The amplicons were digested with EcoRI and NcoI, and cloned together with an NcoI–XbaI fragment representing GFP and the Crb 3′UTR [derived from pUAST-CrbextraTM-GFP (50)] into the pUASTattB vector. For expression in S2R$^+$ cells, the pUAST-based constructs were used together with pAct5-GAL4 (FlyBase ID: FBal0097155).

The cDNA for *Drosophila* Sec24CD was obtained by RT-PCR (5′-AGATCTCGAGATGAATCCGAATATG-3′ and 5′-CGCGGTACCC TAACTCAGCAGATCC-3′) using mRNA prepared from adult flies and subsequently ligated into pEGFP-C3 (Clontech). By PCR using the primer 5′-TATGCGGCCGCCGAGGCCACCATGGTGAGCAAGGGCGAGGA -3′ and 5′-CGCGGTACCCTAACTCAGCAGATCC-3′, a NotI and a KpnI site were introduced and used for cloning GFP-Sec24CD into pUAST. The cDNA for *Drosophila* Sar1 was obtained by RT-PCR (5′-TCCCCGGAATTCATGTTCATCTGGGACTGG-3′ and 5′-CCGCTCGAGTTAATCGATATACTGCGCCAG-3′) using mRNA prepared from adult flies and subsequently ligated into pGEX-6P (GE Healthcare Life Science) expression vector for expression as GST fusion protein in *E. coli*. The Sar1^{H74G} mutant was generated by overlap extension PCR using the primer 5′-ACTTGGGTGGCGGCACTCAGGCACG-3′ and 5′-CGTGCCTGAGTGCCGCCACCCAAGT-3′, each in combination with the primer used for cDNA amplification. Each construct was sequenced for confirmation of its identity.

Embryo collection and immunohistochemistry

Embryo collection, fixation and antibody staining were conducted as described in Ref. 51. The primary antibodies used are stated above. The secondary antibodies used in this study were conjugated to Alexa Fluor-488, −568 and −647 (Life Technologies). Stained embryos were mounted in glycerol-propyl gallate (75% glycerol, 50 mg/mL propyl gallate) and imaged at room temperature on a confocal microscope with a Zeiss Plan-Neofluar 100×/1.3 NA oil objective (LSM 510 controlled by ZEN software, Carl Zeiss). Images were further processed with Fiji and Adobe Illustrator CS5.

Cell culture and transfection

S2R$^+$ cells (Drosophila Genomics Resource Center, stock no. 150) were grown in Schneider's insect medium (Sigma-Aldrich) supplemented with heat-inactivated fetal calf serum (Sigma-Aldrich) at 24°C. Cells were controlled for the absence of mycoplasma using standard PCR. Transfection of S2R$^+$ was done with FuGENE® HD Transfection Reagent (Promega) as suggested by the manufacturer applying the plasmids pAct5C-GAL4 together with pUAST-based, Crb-encoding plasmids. As control, pAct5C-GAL4 was used alone. Cells were harvested 72 h after transfection.

Metabolic labeling and enzymatic removal of glycans

Cells were depleted of methionine and cysteine for 2 h [Schneider's *Drosophila* medium without methionine and glutamine (PAN Biotech) supplemented with 2 mM L-glutamine and 10% fetal calf serum dialysed against PBS to remove small molecules up to 12 kD]. Labeling was done with 25 µCi/mL Met-[^{35}S]-label (Hartmann) for 1 h, followed by various periods of time as detailed in the figure legends. Cells were lysed in 1% Triton X-100 containing lysis buffer [100 mM Pipes, pH 6.8; 120 mM NaCl; 1.5 mM $MgCl_2$; 3 mM $CaCl_2$; 1% (v/v) Triton X-100; 10% (v/v) glycerol; 1 mM phenylmethylsulfonyl fluoride; 1× Complete™ (Roche)] for 10 min at 4°C. Non-solubilized material was separated by centrifugation (10 000 × *g*, 10 min, 4°C). For immunoprecipitation, cell lysates were diluted 1:1 with PNTG buffer [50 mM Pipes, pH 6.8; 120 mM NaCl; 10% (v/v) glycerol; 0.1% (v/v) Triton X-100, 3 mM $CaCl_2$], and protein A/G-agarose beads (Roche) as well as anti-HA/GFP antibodies were added. Samples were rotated for 16 h, and the beads were washed twice with PNTG buffer and once with PN buffer (50 mM Pipes, pH 6.8; 120 mM NaCl). Endoglycosidase H (Endo H) treatment was done as suggested by the manufacturer (New England Biolabs). Proteins were boiled and separated by SDS–PAGE. Gels were fixed (30 min in 40% methanol, 10% acetic acid), dried and analyzed by phosphorimaging (Typhoon FLA 9500; GE Healthcare Life Sciences).

Co-immunoprecipitation

To measure the interaction between Sec24CD and the different HA-Crb-short versions, S2R$^+$ cells expressing the respective proteins

were lysed as described above. The lysates were used for co-immunoprecipitation with 2 μg anti-HA antibodies and protein G-agarose beads (Roche) for 16 h at 4°C. The beads were washed three times with PNTG buffer (see above) and once with HN buffer (50 mM Hepes, pH 7.5; 150 mM NaCl). Immunoprecipitated proteins were boiled with SDS gel loading buffer for 10 min at 65°C, separated by SDS–PAGE, and blotted on nitrocellulose. Blots were blocked and incubated with antibody with 5% BSA (Serva) in 1× TBS-T (50 mM Tris–HCl, pH 7.5; 150 mM NaCl; 5 mM EDTA, pH 8.0; 0.2% Tween). For detection, an anti-GFP antibody (1:5000) and an anti-HA antibody (1:2000) were used as primary and a goat anti-rabbit and anti-mouse antibody conjugated with peroxidase (1:10 000; Sigma-Aldrich) were used as secondary antibodies. Immunodetection was done with ECL chemiluminescence blotting substrate (GE Healthcare Life Sciences).

Sar1 expression and purification

Expression constructs were transformed into *E. coli* strain BL21 DE3. Cells were grown to OD_{600} 0.6–0.8 at 37°C, induced using 0.1 mM IPTG for 4 h at 30°C and lysed with an Emulsiflex Homogenizer. Lysates were centrifuged for 30 min at 4°C and 12 000 × *g*, and the supernatant was loaded on a glutathione sepharose column for gravity flow. GST-Sar1^{H74G} was eluted with 10 mM reduced glutathione (GE Healthcare Life Sciences) in 50 mM Tris, pH 8.0. Elution fractions were analyzed by SDS–PAGE and pooled.

Interaction between Sar1^{H74G} and HA-Crb-short

S2R^{+} cells expressing HA-Crb-short or HA-Crb-short$^{RNKR>MNEP}$ were lysed as described before, and incubated with GST-Sar1 (2 μg) and glutathione-sepharose 4B beads (GE Healthcare Life Science). Bound proteins were analyzed by SDS–PAGE and immunoblotting as described above. For detection an anti-HA antibody (1:5000) was used as primary and a goat anti-mouse antibody conjugated with peroxidase (1:10 000) (Sigma-Aldrich) was used as secondary antibody.

In silico analyses

The annotated Crb sequences were retrieved from FlyBase (http://flybase.org) and the UniProt accession numbers are given in the figure legend. The alignment was obtained using ClustalW. Densitometric analyses were performed with the ImageQuant TL software for 1D gel analysis v8.1 (GE Healthcare Life Sciences). For statistical analyses, two-tailed *t*-tests for unpaired samples were applied using Excel (Microsoft Office 2011, version 14.01.3).

Acknowledgments

We thank Petra Franzmann for purification of GST-Sar1 and Sven Ssykor for injection of *Drosophila* embryos. We acknowledge Marino Zerial and Kai Simons for helpful comments on the manuscript. We thank the fly facility, the light microscopy facility, the sequencing facility, and the radiation safety deputies at MPI-CBG for technical support. We thank the Bloomington *Drosophila* Stock Center for fly stocks, the Developmental Studies Hybridoma Bank (DSHB) for antibodies and the Drosophila Genomics Resource Center (DGRC) for cell lines. This work was supported by the Max-Planck Society (MPG).

GLOSSARY

COPII : coat protein complex II
Crb : Crumbs
C-terminal : carboxy-terminal
EGF : epidermal growth factor
Endo H : Endoglycosidase H
FERM : 4.1/Ezrin/Radixin/Moesin
N-terminal : amino-terminal
PDZ : (PSD-95/Dlg/ZO-1)
S2R^{+} : Schneider cells
TM : transmembrane
UAS : upstream activating sequence

References

1. Bulgakova NA, Knust E. The Crumbs complex: from epithelial-cell polarity to retinal degeneration. J Cell Sci 2009;122:2587–2596.
2. Laprise P, Tepass U. Novel insights into epithelial polarity proteins in Drosophila. Trends Cell Biol 2011;21:401–408.
3. Tepass U. The apical polarity protein network in Drosophila epithelial cells: regulation of polarity, junctions, morphogenesis, cell growth, and survival. Annu Rev Cell Dev Biol 2012;28:655–685.
4. Klebes A, Knust E. A conserved motif in Crumbs is required for E-cadherin localisation and zonula adherens formation in Drosophila. Curr Biol 2000;10:76–85.
5. Wodarz A, Hinz U, Engelbert M, Knust E. Expression of crumbs confers apical character on plasma membrane domains of ectodermal epithelia of Drosophila. Cell 1995;82:67–76.
6. Muschalik N, Knust E. Increased levels of the cytoplasmic domain of Crumbs repolarise developing Drosophila photoreceptors. J Cell Sci 2011;124:3715–3725.
7. Genevet A, Tapon N. The Hippo pathway and apico-basal cell polarity. Biochem J 2011;436:213–224.
8. Blankenship JT, Fuller MT, Zallen JA. The Drosophila homolog of the Exo84 exocyst subunit promotes apical epithelial identity. J Cell Sci 2007;120:3099–3110.
9. Campbell K, Knust E, Skaer H. Crumbs stabilises epithelial polarity during tissue remodelling. J Cell Sci 2009;122:2604–2612.
10. Harris KP, Tepass U. Cdc42 and vesicle trafficking in polarized cells. Traffic 2010;11:1272–1279.
11. Pocha SM, Wassmer T, Niehage C, Hoflack B, Knust E. Retromer controls epithelial cell polarity by trafficking the apical determinant Crumbs. Curr Biol 2011;21:1111–1117.
12. Roeth JF, Sawyer JK, Wilner DA, Peifer M. Rab11 helps maintain apical crumbs and adherens junctions in the Drosophila embryonic ectoderm. PLoS One 2009;4:e7634.

13. Zhou B, Wu Y, Lin X. Retromer regulates apical-basal polarity through recycling Crumbs. Dev Biol 2011;360:87–95.
14. Lee MC, Miller EA, Goldberg J, Orci L, Schekman R. Bi-directional protein transport between the ER and Golgi. Annu Rev Cell Dev Biol 2004;20:87–123.
15. Brandizzi F, Barlowe C. Organization of the ER-Golgi interface for membrane traffic control. Nat Rev Mol Cell Biol 2013;14: 382–392.
16. Barlowe C, Orci L, Yeung T, Hosobuchi M, Hamamoto S, Salama N, Rexach MF, Ravazzola M, Amherdt M, Schekman R. COPII: a membrane coat formed by Sec proteins that drive vesicle budding from the endoplasmic reticulum. Cell 1994;77:895–907.
17. Barlowe C, Schekman R. SEC12 encodes a guanine-nucleotide-exchange factor essential for transport vesicle budding from the ER. Nature 1993;365:347–349.
18. Kuge O, Dascher C, Orci L, Rowe T, Amherdt M, Plutner H, Ravazzola M, Tanigawa G, Rothman JE, Balch WE. Sar1 promotes vesicle budding from the endoplasmic reticulum but not Golgi compartments. J Cell Biol 1994;125:51–65.
19. Miller EA, Beilharz TH, Malkus PN, Lee MC, Hamamoto S, Orci L, Schekman R. Multiple cargo binding sites on the COPII subunit Sec24p ensure capture of diverse membrane proteins into transport vesicles. Cell 2003;114:497–509.
20. Wendeler MW, Paccaud JP, Hauri HP. Role of Sec24 isoforms in selective export of membrane proteins from the endoplasmic reticulum. EMBO Rep 2007;8:258–264.
21. Giraudo CG, Maccioni HJ. Endoplasmic reticulum export of glycosyltransferases depends on interaction of a cytoplasmic dibasic motif with Sar1. Mol Biol Cell 2003;14:3753–3766.
22. Tepass U, Knust E. Phenotypic and developmental analysis of mutations at the crumbs locus, a gene required for the development of epithelia in Drosophila melanogaster. Roux's Arch Dev Biol 1990;199:189–206.
23. Tsarouhas V, Senti KA, Jayaram SA, Tiklova K, Hemphala J, Adler J, Samakovlis C. Sequential pulses of apical epithelial secretion and endocytosis drive airway maturation in Drosophila. Dev Cell 2007;13:214–225.
24. Zhu MY, Wilson R, Leptin M. A screen for genes that influence fibroblast growth factor signal transduction in Drosophila. Genetics 2005;170:767–777.
25. Norum M, Tang E, Chavoshi T, Schwarz H, Linke D, Uv A, Moussian B. Trafficking through COPII stabilises cell polarity and drives secretion during Drosophila epidermal differentiation. PLoS One 2010;5:e10802.
26. Forster D, Armbruster K, Luschnig S. Sec24-dependent secretion drives cell-autonomous expansion of tracheal tubes in Drosophila. Curr Biol 2010;20:62–68.
27. Bonifacino JS, Glick BS. The mechanisms of vesicle budding and fusion. Cell 2004;116:153–166.
28. Standley S, Roche KW, McCallum J, Sans N, Wenthold RJ. PDZ domain suppression of an ER retention signal in NMDA receptor NR1 splice variants. Neuron 2000;28:887–898.
29. Sato K, Otsu W, Otsuka Y, Inaba M. Modulatory roles of NHERF1 and NHERF2 in cell surface expression of the glutamate transporter GLAST. Biochem Biophys Res Commun 2013;430:839–845.
30. Kornfeld R, Kornfeld S. Assembly of asparagine-linked oligosaccharides. Annu Rev Biochem 1985;54:631–664.
31. Maley F, Trimble RB, Tarentino AL, Plummer TH Jr. Characterization of glycoproteins and their associated oligosaccharides through the use of endoglycosidases. Anal Biochem 1989;180:195–204.
32. ten Hagen KG, Zhang L, Tian E, Zhang Y. Glycobiology on the fly: developmental and mechanistic insights from Drosophila. Glycobiology 2009;19:102–111.
33. Benting J, Lecat S, Zacchetti D, Simons K. Protein expression in Drosophila Schneider cells. Anal Biochem 2000;278:59–68.
34. Franke M, Braulke T, Storch S. Transport of the GlcNAc-1-phosphotransferase alpha/beta-subunit precursor protein to the Golgi apparatus requires a combinatorial sorting motif. J Biol Chem 2013;288:1238–1249.
35. Dong C, Nichols CD, Guo J, Huang W, Lambert NA, Wu G. A triple arg motif mediates alpha(2B)-adrenergic receptor interaction with Sec24C/D and export. Traffic 2012;13:857–868.
36. Farhan H, Reiterer V, Korkhov VM, Schmid JA, Freissmuth M, Sitte HH. Concentrative export from the endoplasmic reticulum of the gamma-aminobutyric acid transporter 1 requires binding to SEC24D. J Biol Chem 2007;282:7679–7689.
37. Paulhe F, Imhof BA, Wehrle-Haller B. A specific endoplasmic reticulum export signal drives transport of stem cell factor (Kitl) to the cell surface. J Biol Chem 2004;279:55545–55555.
38. Kumichel A, Knust E. Apical localisation of crumbs in the boundary cells of the Drosophila hindgut is independent of its canonical interaction partner stardust. PLoS One 2014;9:e94038.
39. Dunin-Borkowski OM, Brown NH. Mammalian CD2 is an effective heterologous marker of the cell surface in Drosophila. Dev Biol 1995;168:689–693.
40. Ivan V, de Voer G, Xanthakis D, Spoorendonk KM, Kondylis V, Rabouille C. Drosophila Sec16 mediates the biogenesis of tER sites upstream of Sar1 through an arginine-rich motif. Mol Biol Cell 2008;19:4352–4365.
41. Springer S, Schekman R. Nucleation of COPII vesicular coat complex by endoplasmic reticulum to Golgi vesicle SNAREs. Science 1998;281:698–700.
42. Kondylis V, Rabouille C. The Golgi apparatus: lessons from Drosophila. FEBS Lett 2009;583:3827–3838.
43. Shivas JM, Morrison HA, Bilder D, Skop AR. Polarity and endocytosis: reciprocal regulation. Trends Cell Biol 2010;20:445–452.
44. Venditti R, Wilson C, De Matteis MA. Exiting the ER: what we know and what we don't. Trends Cell Biol 2014;24:9–18.
45. Campos-Ortega JA, Hartenstein V. The Embryonic Development of *Drosophila melanogaster*. Berlin: Springer; 1997.
46. Venken KJ, Bellen HJ. Transgenesis upgrades for Drosophila melanogaster. Development 2007;134:3571–3584.
47. Bachmann A, Grawe F, Johnson K, Knust E. Drosophila Lin-7 is a component of the Crumbs complex in epithelia and photoreceptor

cells and prevents light-induced retinal degeneration. Eur J Cell Biol 2008;87:123–136.
48. Richard M, Grawe F, Knust E. DPATJ plays a role in retinal morphogenesis and protects against light-dependent degeneration of photoreceptor cells in the Drosophila eye. Dev Dyn 2006;235:895–907.
49. Bischof J, Maeda RK, Hediger M, Karch F, Basler K. An optimized transgenesis system for Drosophila using germ-line-specific phiC31 integrases. Proc Natl Acad Sci USA 2007;104:3312–3317.
50. Pellikka M, Tanentzapf G, Pinto M, Smith C, McGlade CJ, Ready DF, Tepass U. Crumbs, the Drosophila homologue of human CRB1/RP12, is essential for photoreceptor morphogenesis. Nature 2002;416: 143–149.
51. Klose S, Flores-Benitez D, Riedel F, Knust E. Fosmid-based structure-function analysis reveals functionally distinct domains in the cytoplasmic domain of Drosophila crumbs. G3 (Bethesda) 2013;3:153–165.